European Commission
Energy, Environment
and Sustainable
Development

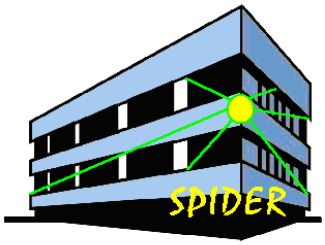

EVG1-CT-1999-00013 SPIDER

WORKPACKAGE 8 – TASKS 8.1 & 8.2

Deliverable D17

Design procedures for damped cable system implementation

Stefano SORACE
(Università di Udine)
Gloria TERENZI
(Università di Firenze)

EVG1-CT-1999-00013 SPIDER/8.1/ UDINE/SSO/03/VF-C

August 2002

1. INTRODUCTION

This report describes a specially conceived procedure for the design of the damped cable system (DCS). The procedure is formulated according with a performance-based non-linear dynamic approach, and consists of a preliminary and a final verification phases.

The former phase is carried out by referring first to a modal transformation, and then to a single-degree-of-freedom (SDOF) dynamic idealisation of the building protected by DCS. Both schemes derive from simplified assumptions on the structural characteristics and the cable geometry, as well as on the design hypothesis of preserving a first mode-dominated seismic response also in protected conditions. The cable geometry is traced out at this stage of the analysis with the aim of approaching – within the limits imposed by the architectural constraints and the actual structural configuration – a parabolic layout, or the "constant horizontal force" one. In fact, these represent the two most performing shapes highlighted by the extensive parametric analyses carried out by Udine University team within the context of Work-Package 1, as well as in the subsequent numerical investigations developed on selected case studies [1-3].

The solving equations of motion are explicitly formulated for the non-linear dynamic SDOF problem, which can nevertheless be modelled also by commercial calculus programs including non-linear viscous dashpot elements in their basic libraries, among which the widely used SAP2000NL code.

The four-step preliminary phase is carried out by referring to the highest hazard level assumed in the performance-based approach, although additional checks can also be developed with regards to the remaining levels. The procedure is started by imposing a target reduction on the fundamental period of the unprotected structure, from which the preliminary values of cable-section area, and of first and second-branch Jarret device stiffness are determined (steps 1 and 2). The cable and device pre-loads are then evaluated by a separate criterion, where the limit top displacement of the building deemed compatible with the highest hazard level-related design objective is input (step 3). The preliminary choice of the damping coefficient of Jarret device is finally located by a parametric enquiry based on the proposed dynamic SDOF model (step 4).

By collecting these data, the final verification phase is afterwards developed by the complete structural model of the building, or a representative portion of it (e.g., in the case of a multi-

frame structure composed by a series of equally spaced identical frames, only one frame can be analysed, by considering its pertinent area for vertical and seismic loads.) For all cases where a two-dimensional schematisation provides an effective simulation of the dynamic problem, the model can be generated by the finite element program "J2d", expressly elaborated by Udine University within this Project [1], [4]. A three-dimensional model can otherwise be produced by means of the ABAQUS code, by following either the most sophisticated [5] or the simplified [6] approaches proposed by ENEA team as regards the sliding contact between cable and floor slabs. Simplified models based on the same criteria proposed in [6] are currently under implementation within more accessible commercial calculus programs.

By integrating the single objective basically posed in the preliminary phase, a multiple design objective is formulated in the verification stage, for which three (or at least two) performance levels are to be met in correspondence with three (or two) pre-fixed earthquake levels, whose hazards are expressed in terms of probability of exceedance in a given return period. The required performances are typically assessed in terms of deformation parameters. Relevant evaluation criteria and limitations are derived herein from a critical review of leading international guidelines for the design of new structures, or the rehabilitation of existing ones. In the case of retrofit designs, a strength-based control of response is also conducted, so as to quantify the additional stress states induced by the action of cables – both in static and seismic conditions – into the existing structural members. Proper strengthening measures are then adopted for members where the calculated stress states are not admissible. For new designs, the combined deformation/strength-based control of response directly leads to the final proportioning of the entire structural system.

A demonstrative application of the design procedure is presented in the final section of this report for two retrofit case studies, represented by a seven-story steel and a three-story R/C non-seismically designed office buildings.

2. PERFORMANCE-BASED DESIGN APPROACH

A unified performance-based approach is followed, for retrofit and new designs. According to this approach – typically adopted within a seismic rehabilitation context by FEMA 273/274

[7], [8] and ATC-40 [9], or in new design by SEAOC 2000 [10] – a multiple design objective is formulated, for which a "Life Safety" (LS) and a "Collapse Prevention" (CP) performance levels are pursued in correspondence with the "Basic Design Earthquake" (BDE) and the "Maximum Considered Earthquake" (MCE), respectively. A 10%, and 2% probabilities of exceedance over a return period T_r of 50 years are assigned to BDE, and MCE, respectively. In addition to this double objective, a third one can be optionally assumed, represented by the attainment of an Immediate Occupancy (IO) level under the action of a reduced seismic event, defined as "Serviceability Earthquake" (SE). The SE probability of exceedance over T_r is fixed at 50%. This third objective is aimed at ensuring a totally elastic structural response, as well as at preventing damage to non-structural members interacting with the lateral load-resisting system (essentially masonry infills), for low-hazard events.

Many different values of limitations to the response deformation-parameters are imposed by documents [7-10], as well as by other assessment and design guidelines, with regards to the above-mentioned performance levels, depending on building materials, structural conception and characteristics, building function, etc. Moreover, when special seismic protection systems are incorporated within the main structure, a proper calibration of limitations is required, to take into account the higher performance potentialities ensured by these supplemental systems in comparison with traditional designs or retrofits. In doing so, an enhanced design objective is implicitly assumed, which is obtained by shifting the limitations relevant to any single performance level to the lower one (e.g., the acceptable drift values for LS, to CP; the IO-ones, to LS; etc), except for possible adjustments established case by case by the designer. This allows justifying the additional costs, as well as the higher know-how and implementation works entailed by the adoption of advanced protection strategies.

By focusing on R/C and steel framed buildings, a review of limitations in terms of inter-story drift (I_d) led to select – in accordance with the enhanced-performance view above – the "admissible" values summed up in Table 1, where symbols denote presence (NS) or not (S) of interacting non-structural infill panels. When referring to the NS limits, the structural model should consistently include the response contribution (hysteretic in case of non-linear dynamic analyses) of infills. However, this contribution remarkably influences the peak-response parameters until the panels behave elastically, that is, at most for serviceability-type events. Thus, a SE-related performance-control requires modelling also the effects of infills. On the other hand, when a pronounced plastic response of panels is induced – as typically

occurs for the BDE and MCE levels of action – a notably lower influence on the most severe response phases is observed. This is due to the quickly degrading stiffness and strength properties of masonry panels, compared to the more stable hysteretic characteristics of the frame members, which drastically reduce the contribution of infills in these phases.

Performance Level	I_d (%)
NS-CP	1
NS-LS	0.5
NS-IO	0.2
S-CP	2
S-LS	1
S-IO	0.4

Table 1. Enhanced design objective-related inter-story drift limitations selected for R/C and steel framed buildings

Therefore, the NS-LS and NS-CP thresholds reported in Table 1, which are aimed at ensuring repairable damage (NS-LS) and prevention from collapse (NS-CP) of infills, can also be kept in practice without including panels in the structural model, when BDE or MCE-type actions are considered.

The deformation-based control of performance is completed by a series of complementary checks, essentially carried out in terms of maximum elastic or plastic beam and column-section rotations. Reference is made again to documents [7-10] for detailed information about relevant limitations.

3. PRELIMINARY DESIGN PHASE OF DCS

The preliminary design phase (PDP) is subdivided in the four procedural steps described below. The following lower indices:

“d” for damper;

"c" for cable;

"s" for structure;

"dc" for damped cable;

"sdc" for structure equipped with damped cable;

and upper indices:

"t" for tentative (i.e., first tentative assumption in PDP);

"p" for preliminary (i.e., resulting value from PDP);

"h" for horizontal (i.e., projection along the horizontal axis),

are applied to the involved mechanical parameters, that is:

K_{d1}, K_{d2} = stiffness values characterising the first (i.e., below the pre-load threshold) and second (beyond pre-load) response branches of Jarret device;

F_{d0} = pre-load imposed to Jarret device;

C = damping coefficient of Jarret device;

A_c = cable-section area;

F_{c0} = pre-load applied to cable.

Step 1

• Searched parameters: the tentative values of K_{d2}, K_c (K_{d2}^t, K_c^t), and the preliminary value of A_c (A_c^p).

A modal analysis of the single frame for which a couple of cables is being designed is carried out, to evaluate its fundamental vibration period T_{1s} and the effective mass coefficient for the first mode, α_1.

The latter value is then multiplied by the total frame weight W_s, so as to obtain the transformed weight, W_s^{m1}

$$W_s^{m1} = \alpha_1 \cdot W_s \tag{1}$$

and the corresponding elastic stiffness, K_s^{m1}

$$K_s^{m1} = \frac{4\pi^2 \cdot W_s^{m1}}{T_{1s}^2 \cdot g} \tag{2}$$

for an equivalent SDOF-system representation of the first mode of vibration of the frame.
For regular buildings (i.e., with uniform mass distribution along the height, and straight line mode shapes), a quicker first-mode transformation can be drawn by an approximate α_1 estimate based on the number of building stories. Suggested values [10] are reported in Table 2.

Number of stories	α_1
1	1
2	0.9
3	0.86
5	0.82
10	0.78

Table 2. Approximate α_1 coefficients for regular buildings

The first objective of the design procedure consists in reducing the fundamental vibration mode of the frame to a pre-fixed fraction $T_{1\mathrm{sdc}}^{\mathrm{t}}$

$$T_{1\mathrm{sdc}}^{\mathrm{t}} = \beta \cdot T_{1\mathrm{s}} \tag{3}$$

after the incorporation of DCS. The β coefficient is a free parameter to be established by the designer. As a general suggestion drawn from the examined case studies, reference can be made to β values around 0.8, when the bare frame is not very flexible, that is, approximately for $T_{1\mathrm{s}} \leq 1\,\mathrm{s}$. Lightly lower β values can be tentatively adopted otherwise, with a lower limit of 0.65÷0.7, below which the dimensions of damped cable tend to increase excessively. On the other hand, no actual benefits can be obtained from DCS application to stiff frames ($T_{1\mathrm{s}} \leq 0.5\,\mathrm{s}$).
The tentative value of the horizontal projection of DC stiffness, $K_{\mathrm{dc}}^{\mathrm{t,h}}$ is derived from the $T_{1\mathrm{sdc}}^{\mathrm{t}}$ expression

$$T_{1sdc}^{t} = \beta \cdot T_{1s} = 2\pi \sqrt{\frac{W_s^{m1}}{g(K_s^{m1} + K_{dc}^{t,h})}} \tag{4}$$

where g is the acceleration of gravity, as:

$$K_{dc}^{t,h} = \frac{4\pi^2 \cdot W_s^{m1}}{g(\beta \cdot T_{1s})^2} - K_s^{m1} \tag{5}$$

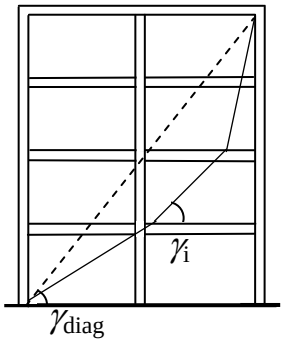

Figure. 1. Diagonal approximation of cable layout within step 1 of PDP

The tentative DC axial stiffness is initially computed by referring to an approximated diagonal shape of the cable (Fig. 1), which gives

$$K_{dc}^{t} = \frac{K_{dc}^{t,h}}{\cos\gamma_{diag}} \tag{6}$$

Under the hypothesis of assigning equal stiffness to device (second response branch) and cable, their analytical in-series combination

$$\frac{1}{K_{d2}^{t}} + \frac{1}{K_{c}^{t}} = \frac{1}{K_{dc}^{t}} \tag{7}$$

allows providing the searched tentative values K_{d2}^{t}, K_{c}^{t} from (6):

$$K_{d2}^{t} = K_{c}^{t} = 2K_{dc}^{t} \tag{8}$$

The actual cable layout is traced out at this point, and the total cable length L_t is calculated as the sum of the inter-story segment-lengths L_i. The tentative cable area A_c^t is then deduced as:

$$A_c^t = \frac{K_c^t \cdot L_t}{E_s} \tag{9}$$

being E_s the Young modulus of steel. The A_c^t estimate is subsequently transformed in the closest area resulting from the assemblage of groups of seven or twelve 0.6-inches strands, A_c^p, which represents the preliminary A_c design value.

Step 2

- Check on parameter values determined in step 1: K_{d2}^t, K_c^t, A_c^p.
- Searched parameters: the preliminary values of K_{d2}, K_{d1}, K_c (K_{d2}^p, K_{d1}^p, K_c^p).

The tentative K_c^t value, quickly estimated by (6) to speed calculations in step 1, is herein turned into the resulting PDP value K_c^p, based on the A_c^p area as well as the exact cable layout. Said $K_{ci}^p = \frac{E_s \cdot A_c^p}{L_i}$ the axial stiffness of the *i*th inter-story segment of cable, the searched K_c^p parameter is obtained as:

$$K_c^p = \left(\sum_i \frac{1}{K_{ci}^p} \right)^{-1} \tag{10}$$

The horizontal component $K_c^{p,h}$ is then calculated from the corresponding projections at each story $K_{ci}^{p,h}$, through relevant angles γ_i (Fig. 1):

$$K_c^{p,h} = \left(\sum_i \frac{1}{K_{ci}^{p,h}} \right)^{-1} \tag{11}$$

By substituting $K_{dc}^{p,h} = \frac{K_c^{p,h}}{2}$ to $K_{dc}^{t,h}$ in (4)

$$T_{1sdc}^{p} = 2\pi \sqrt{\frac{W_s^{m1}}{g(K_s^{m1} + K_{dc}^{p,h})}} \tag{12}$$

the first approximate value of the fundamental vibration period of the frame equipped with DCS, computed in step 1, is checked. If T_{1sdc}^{p} substantially equals T_{1sdc}^{t} – as generally occurs – the preliminarily selected cable area A_c^p is confirmed, and thus also K_c^p (and $K_c^{p,h}$).

From the condition $K_{d2}^{p,h} = K_c^{p,h}$ the preliminary design value of the second-branch device stiffness is also derived

$$K_{d2}^{p} = \frac{K_{d2}^{p,h}}{\cos\gamma_1} \tag{13}$$

A previously proposed [1] empirical relation is afterwards applied to evaluate the first-branch stiffness from K_{d2}^{p}

$$K_{d1}^{p} = 20K_{d2}^{p} \tag{14}$$

When T_{1sdc}^{p} non-negligibly differs from T_{1sdc}^{t}, the initially adopted number of strands has to be changed, and step 2 consequently repeated with the modified A_c^p value, until the target β reduction of fundamental vibration period is reached.

Step 3

• Searched parameters: the preliminary values of $F_{c0,} F_{d0}$ (F_{c0}^{p}, F_{d0}^{p}).

The preliminary value of cable pre-load is evaluated by the following formula:

$$F_{c0}^{p} = \frac{K_c^p \cdot \Delta L_c}{\eta} \tag{15}$$

where ΔL_c is the cable stretch corresponding to a pre-fixed value of the building roof (or of the cable upper anchorage floor) displacement d_r, and η is a free parameter. Equation (15) automatically provides also F_{d0}^{p}, since by hypothesis $F_{d0}^{p} = F_{c0}^{p}$.

When a multiple performance objective is assumed, the reference d_r limit value must be calibrated against the most severe seismic level involved in the design process (i.e., MCE, for SE-BDE-MCE or BDE-MCE combinations; and BDE, for a SE-BDE one). As way of example, if the highest hazard is represented by MCE and the corresponding performance by NS-CP, by referring to the limits in Table 1 and hypothesising an approximately uniform seismic response along the building height H, d_r can be set as equal to 0.01 H.

Also η must be tuned on the most severe earthquake level. However, the best calibration of this coefficient is obtained by directly considering its influence on F_{d0}, rather than on F_{c0}. In particular, to account for the non-linear proportion among the damping actions produced by a Jarret devices under scaled input levels, the following η choices are suggested: 3, or 4÷5, when BDE, or MCE represents the highest hazard level. These values on average offer a good balance between the needs of keeping cable response always in tension (F_{c0} not too low), and enlarging as much as possible the operation field of device (F_{d0} not too high).

Step 4

- Searched parameter: the preliminary value of C (C^p).

The damping coefficient represents the last mechanical quantity to be preliminarily established. Due to the strong non-linearity of Jarret device damping action, as well as the critical role played by C over the global operation of DCS, a parametric analysis is needed at this stage to locate the best choice of this coefficient. The relevant computation is developed by a set of input accelerograms consistent with a reference response spectrum, and scaled to the most severe hazard level (although this analysis can also involve the remaining hazard levels, to obtain a first global view of the system capacities). At least four input signals must be assumed, so as to provide statistical significance to the results of the non-linear dynamic enquiry [1-4]. Unless differently recommended, the response can be elaborated in mean terms over the set of selected accelerograms.

In order to speed up the numerical analysis, a SDOF dynamic model is to be preferably used, by postponing the analyses with the complete structural model to the final verification phase. The assembled SDOF model is graphed in Fig. 2, where the parameters fixed in steps 1 through 3 are introduced. Further symbols in Fig. 2 represent: M_s^{m1} the first mode-equivalent building mass ($M_s^{m1} = \frac{W_s^{m1}}{g}$); M_f = 0 a fictitious mass that allows attaining the desired in-

series connection of the four involved spring elements; and K_f the stiffness of the fictitious spring linked to M_f, which provides K_c^p in combination with K_m, as:

$$\frac{1}{K_f}+\frac{1}{K_m}=\frac{1}{K_s^{m1}} \tag{16}$$

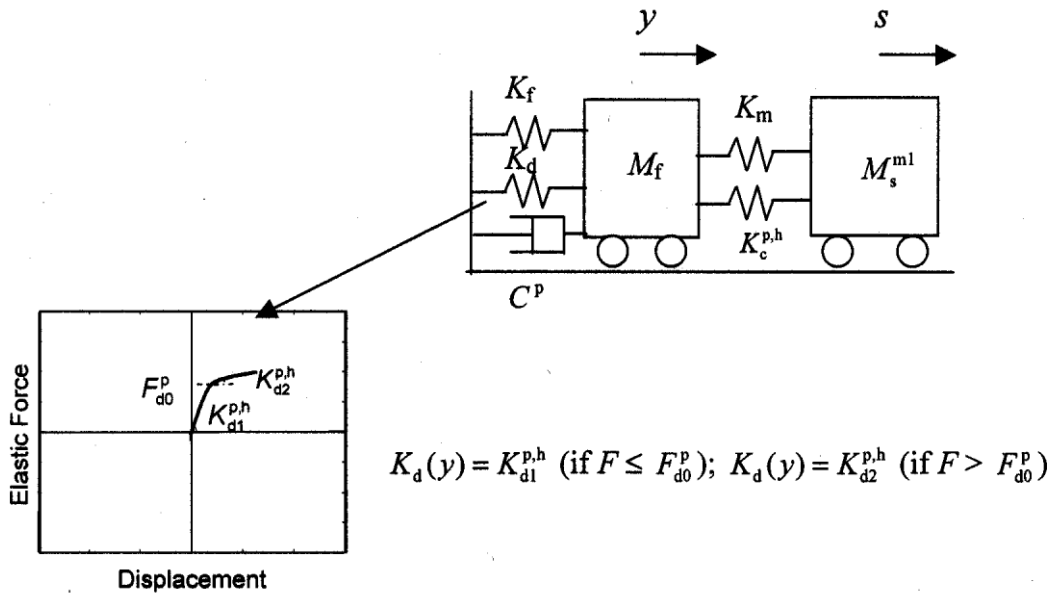

Figure 2. SDOF dynamic system adopted for parametric investigation on damping coefficient

In particular, the best simulation of the actual structural problem is obtained by imposing $K_f = 3\,K_m$ in (16).

The dynamic SDOF model shown in Fig. 2 can be reproduced by commercial finite element programs including non-linear viscous dashpot elements in their libraries, among which the SAP2000NL code [11], in widespread use within the professional community. Nevertheless, to allow a direct analytical solution be drawn by simple mathematical tools (e.g., like the basic-math solvers incorporated in MATLAB, EXCEL, etc), the solving equations of this problem are also expressly formulated in the following.

By referring to Fig. 2, the dynamic equilibrium relations for an input acceleration $\ddot{u}_g$ are:

$$M_f\ddot{y}+C^p\,\mathrm{sign}(\dot{y})|\dot{y}|^{\alpha}+F_d+K_f y-K_c^{p,h}s-K_m s=-M_f\ddot{u}_g \tag{17}$$

$$M_s^{m1}\ddot{y}+M_s^{m1}\ddot{s}+(K_c^{p,h}+K_m)s=-M_s^{m1}\ddot{u}_g \tag{18}$$

where $\mathrm{sign}(\bullet)$ represent the signum function, $|\bullet|$ the absolute value, and F_{d} is given by

$$F_{\mathrm{d}} = K_{\mathrm{d2}}^{\mathrm{p,h}} x + \frac{(K_{\mathrm{d1}}^{\mathrm{p,h}} - K_{\mathrm{d2}}^{\mathrm{p,h}})\, x}{\left[1 + \left|\frac{K_{\mathrm{d1}}^{\mathrm{p,h}} x}{F_{\mathrm{d0}}^{\mathrm{p}}}\right|^{\mathrm{R}}\right]^{1/\mathrm{R}}} \tag{19}$$

The time variable t is omitted for brevity's sake in (17), (18) and (19), as well as in the following passages. By posing $M_f = 0$ in (17), the dependent coordinate s is obtained as a function of the free coordinate y:

$$C^{\mathrm{p}}\mathrm{sign}(\dot{y})|\dot{y}|^{\alpha} + F_{\mathrm{d}} + K_{\mathrm{f}}\, y = (K_{\mathrm{c}}^{\mathrm{p,h}} + K_{\mathrm{m}})s \quad \Rightarrow \quad s = \frac{1}{K_{\mathrm{c}}^{\mathrm{p,h}} + K_{\mathrm{m}}}(C^{\mathrm{p}}\mathrm{sign}(\dot{y})|\dot{y}|^{\alpha} + F_{\mathrm{d}} + K_{\mathrm{f}}\, y) \tag{20}$$

Then, by substituting s in (18), the resulting equation of motion in y

$$\begin{aligned} &M_{s}^{\mathrm{m1}}\ddot{y} + \frac{M_{\mathrm{s}}^{\mathrm{m1}} C^{\mathrm{p}}}{(K_{\mathrm{c}}^{\mathrm{p,h}} + K_{m} + K_{\mathrm{d}} + K_{\mathrm{f}})}\frac{\mathrm{d}^2\left[\mathrm{sign}(\dot{y})|\dot{y}|^{\alpha}\right]}{\mathrm{dt}^2} + \frac{(K_{\mathrm{c}}^{\mathrm{p,h}} + K_{m})}{(K_{\mathrm{c}}^{\mathrm{p,h}} + K_{m} + K_{\mathrm{d}} + K_{\mathrm{f}})}C^{\mathrm{p}}\mathrm{sign}(\dot{y})|\dot{y}|^{\alpha} + \\ &+ \frac{(K_{\mathrm{c}}^{\mathrm{p,h}} + K_{m})}{(K_{\mathrm{c}}^{\mathrm{p,h}} + K_{m} + K_{\mathrm{d}} + K_{\mathrm{f}})}F_{\mathrm{d}} + \frac{K_{\mathrm{f}}(K_{\mathrm{c}}^{\mathrm{p,h}} + K_{m})}{(K_{\mathrm{c}}^{\mathrm{p,h}} + K_{m} + K_{\mathrm{d}} + K_{\mathrm{f}})}y = -\frac{(K_{\mathrm{c}}^{\mathrm{p,h}} + K_{m})}{(K_{\mathrm{c}}^{\mathrm{p,h}} + K_{m} + K_{\mathrm{d}} + K_{\mathrm{f}})}M_{\mathrm{s}}^{\mathrm{m1}}\ddot{u}_{\mathrm{g}} \end{aligned} \tag{21}$$

is obtained. Elimination of the negligible term $\frac{M_{\mathrm{s}}^{\mathrm{m1}} C^{\mathrm{p}}}{(K_{\mathrm{c}}^{\mathrm{p,h}} + K_{m} + K_{\mathrm{d}} + K_{\mathrm{f}})}\frac{\mathrm{d}^2\left[\mathrm{sign}(\dot{y})|\dot{y}|^{\alpha}\right]}{\mathrm{dt}^2}$ in (21) finally provides the more compact form of the solving equation of motion

$$M_{\mathrm{s}}^{\mathrm{m1}}\ddot{y} + \phi(y)C^{\mathrm{p}}\mathrm{sign}(\dot{y})|\dot{y}|^{\alpha} + \phi(y)F_{\mathrm{d}} + K_{\mathrm{f}}\phi(y)y = -\phi(y)M_{\mathrm{s}}^{\mathrm{m1}}\ddot{u}_{\mathrm{g}} \tag{22}$$

where

$$\phi(y) = \frac{(K_{\mathrm{c}}^{\mathrm{p,h}} + K_{m})}{(K_{\mathrm{c}}^{\mathrm{p,h}} + K_{m} + K_{\mathrm{d}} + K_{\mathrm{f}})} \tag{23}$$

The preliminary C^{p} choice resulting from the parametric enquiry based on (22), or on a finite element model reproducing the assemblage in Fig. 2, should ensure a good balance between

the requests of achieving the target performance of device and at the same time, restraining as much as possible its dimension and cost. This double objective is generally satisfied for a narrow "optimal" C range, below which the device performance can not yet be accepted, and beyond which any further increase of damping coefficient (and thus of device dimension) does not provide appreciable response benefits.

To direct the designer at the beginning of the parametric analysis, the following rough estimates C_i of damping coefficient are suggested to initialise the searching process, as functions of the DCS-pertinent weight W_s:

$C_i \approx 30$ kN/(mm/s)$^\alpha$ for $W_s = 1000 \div 1200$ kN;

$C_i \approx 40$ kN/(mm/s)$^\alpha$ for $W_s = 1500 \div 1800$ kN;

$C_i \approx 50$ kN/(mm/s)$^\alpha$ for $W_s = 2200 \div 2600$ kN;

$C_i \approx 80$ kN/(mm/s)$^\alpha$ for $W_s = 4000 \div 4500$ kN;

$C_i \approx 100$ kN/(mm/s)$^\alpha$ for $W_s = 6000 \div 7000$ kN;

$C_i \approx 120$ kN/(mm/s)$^\alpha$ for $W_s = 8000 \div 10000$ kN.

Obviously, these values are to be intended only as first gross approximations – again for regular framed buildings – starting from which the outcome of the parametric investigation could even decidedly differ. In any case, these estimates must not be regarded as reference terms for comparison with the final results of the entire design procedure.

4. FINAL VERIFICATION DESIGN PHASE OF DCS

The final verification design phase (FVDP) is carried out with the complete structural model of the building, according to the observations reported in section 1.

All parameters resulting from the preliminary design phase are incorporated in the model, which is subjected to the same accelerograms used as input in step 4 of PDP. This final stage of the analysis is aimed at checking the accomplishment of the assumed deformation-based performance objectives, as well as at developing the needed strength-based verifications on the frame and foundation members. These will lead to devise the proper strengthening interventions on possible unsafe elements, in case of retrofit designs; and to directly dimensioning the structural members, when dealing with new designs.

5. DESIGN CASE STUDIES

5.1. Seismic retrofit of a seven-story steel office building

The first case study concerns a steel framed structure representative of a series of early-1970s office buildings in Italy. These buildings were typically designed for vertical and wind loads, and without seismic provisions, according to the Italian technical Standards of those years. The structural skeleton consists of three-span – transversal direction –, seven-span – longitudinal direction – moment-resisting frames with semi-rigid flanged joints, without vertical braces or shear walls, so as to achieve open-space interiors. Light concrete panels interacting with frame members were adopted for infills. Glazed finishes characterise the central portions of the two lateral and two front façades. Glazed panels also surround elevators and stairs.

Due to the subsequent seismic classification of its site, the building appeared as a good pilot-example for a possible retrofit design based on the DCS concept. A schematic transversal view and plan of the structure are shown in Fig. 3. The profiles of columns are summed up in Table 3. All beams are made of HEB 300 profiles.

With the view of preserving the original open-space internal design, it is herein hypothesised of placing a couple of cables only on the four perimeter frames. Proper finishes, like the ones devised within Task 3 of this Project for similar solutions, can provide a pleasant aesthetic impact to the intervention, and a renewed architectural aspect to the building.

The design simulation is conducted with regard to the transversal direction, for which the upper anchorage of the cable is fixed at the fifth floor. In fact, due to an aspect ratio of the structure equal to around 1.8 for this direction, a negligible contribution could be obtained by prolonging the cable up to the seventh story.

An assessment enquiry on the performance capacities of the unprotected structure at the BDE level (characterised by a peak ground acceleration of 0.3 g) highlighted a maximum inter-story drift of 39.8 mm (1.14% of story height), from a conventional elastic analysis, or 49.7 mm (1.42%), from a plastic one. Both data refer to the fourth floor. At the MCE level (peak ground acceleration of 0.6 g) the plastic drift at the same floor reached 71.8 mm (2.05%).

Starting from these results, the design procedure is applied below by following the step-by-step sequence discussed in section 4. Involved equations are also reminded for convenience.

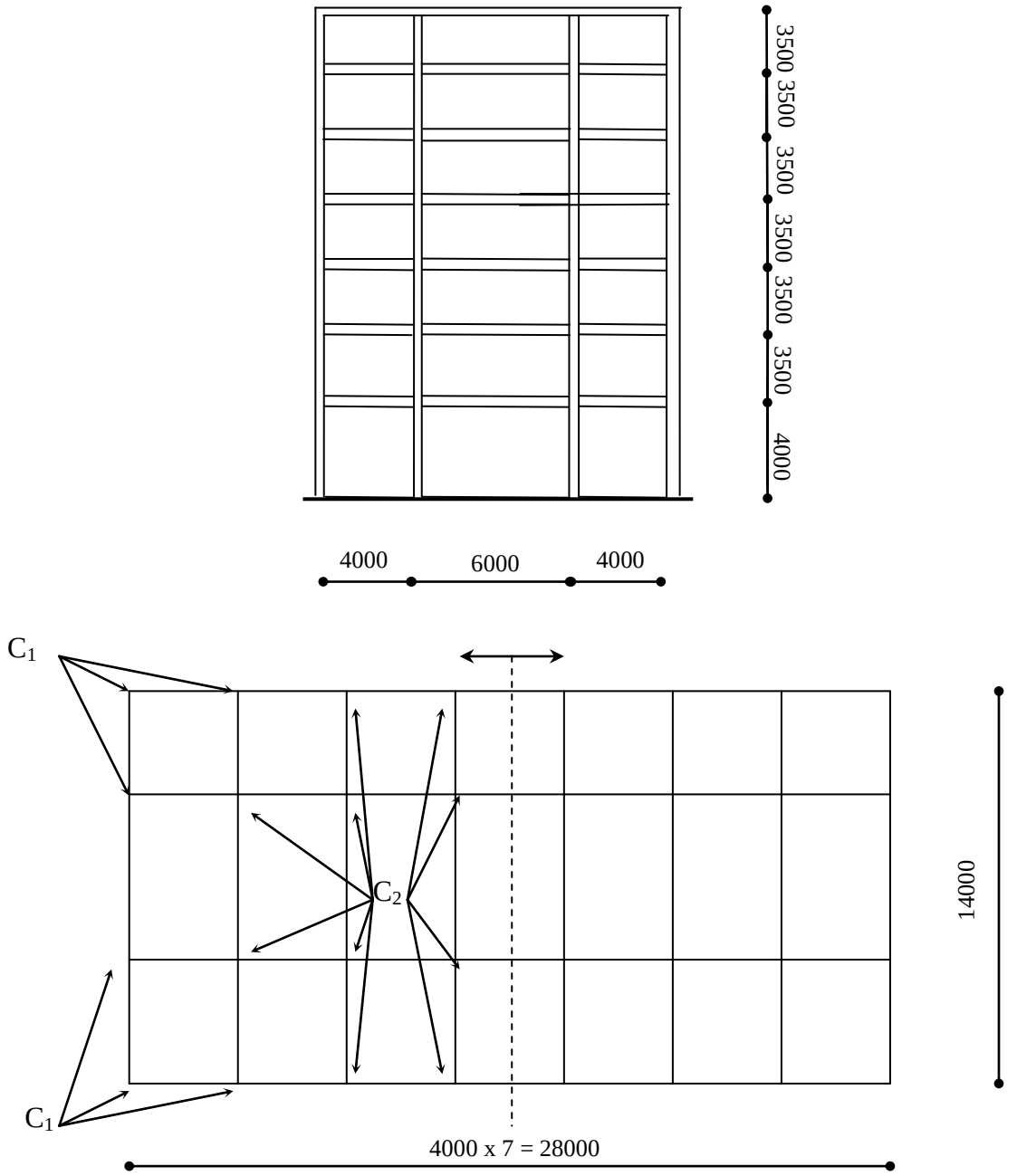

Fig. 3. Schematic transversal view and plan of seven-story steel building (dimensions in millimeters)

Story	C1	C2
1-2	HEB 340	HEB 240
3-4	HEB 280	HEB 180
5-6-7	HEB 240	HEB 180

Table 3. Column profiles

PDP – Step 1

The reference data are: W_s = 9770 kN (corresponding to half structure); T_{1s} = 1.2 s; α_1 = 0.8 (calculated from modal analysis). Then:

(1) $\Rightarrow$ W_s^{m1} = 7816 kN

(2) $\Rightarrow$ K_s^{m1} = 21840 N/mm

By assuming β = 0.8:

(3) $\Rightarrow$ T_{1sdc}^{t} = 0.96 s

(4), (5) $\Rightarrow$ $K_{dc}^{t,h}$ = 12290 N/mm

Being γ_{diag} = 52.1°, from which $\cos\gamma_{diag}$ = 0.614, it follows:

(6) $\Rightarrow$ $K_{dc}^{t} = \dfrac{K_{dc}^{t,h}}{\cos\gamma_{diag}}$ = 20010 N/mm

(8) $\Rightarrow$ $K_{d2}^{t} = K_{c}^{t} = 2K_{dc}^{t}$ = 40020 N/mm

The cable layout is traced out by approaching a parabolic curve, which leads to the geometrical and stiffness data in Table 4.

Floor	L_i (mm)	γ_i (°)	$\cos(\gamma_i)$	K_{ci}^{p} (N/mm)	$K_{ci}^{p,h}$ (N/mm)
1	8276	28.8	0.876	137022	120031
2	4136	57.0	0.544	274178	149153
3	3910	63.4	0.447	290025	129641
4	3910	63.4	0.447	290025	129641
5	3630	74.0	0.275	312397	85909

Table 4. Geometrical and stiffness data of cable

From the L_i values in Table 4, L_t = 23860 mm, and

(9) $\Rightarrow A_c^t = \frac{K_c^t \cdot L_t}{E_s} = 4630 \text{ mm}^2$

derive.

Based on (9), three cables of twelve strands are selected, from which $A_c^p = 5400 \text{ mm}^2$.

PDP – Step 2

(10) $\Rightarrow K_c^p = 47520 \text{ N/mm}$

(11) $\Rightarrow K_c^{p,h} = 23750 \text{ N/mm}$; $K_{dc}^{p,h} = 11875 \text{ N/mm}$

(12) $\Rightarrow T_{1sdc}^p = 0.966 \text{ s}$

T_{1sdc}^p coincides at the second decimal with T_{1sdc}^t, and thus A_c^p is confirmed.

(13) $\Rightarrow \cos\gamma_1 = 0.876$; $K_{d2}^p = 27110 \text{ N/mm}$

(14) $\Rightarrow K_{d1}^p = 542200 \text{ N/mm}$

PDP – Step 3

A drift limit of 1% (NS-CP) is assumed as the basic objective of the retrofit design at the MCE level. By referring to the height of the fifth floor (18 m), d_r = 180 mm is obtained, from which ΔL_c =110 mm. Then:

(15) $\Rightarrow F_{c0}^p = F_{c0}^p = 1306 \text{ kN}$

PDP – Step 4

The non-linear dynamic SDOF analysis developed by the model presented in section 3 provides C^p = 120 kN/(mm/s)$^\alpha$ as the minimum C value for which the imposed 0.5% (NS-LS) and 1% (NS-CP) drift limits are met, for the BDE and MCE input levels, respectively. Moreover, over C^p the response results to be nearly insensitive to further increases of the damping coefficient.

FVDP

The final verification phase, carried out by the "J2d" program, substantially validates the results of the PDP. Maximum inter-story drifts of 16.9 mm (0.48%), and 37.2 mm (0.99%) are found at the BDE, and MCE levels of input action. Therefore, the preliminarily selected values of the design parameters can be definitely accepted in terms of drift performance.
As premised in the previous sections, additional deformation-based controls, as well as all needed strength-based verifications should be carried out at this point, to complete performance assessment, and devise the required strengthening interventions on frame members. These integrative analyses are omitted herein, since they are beyond the scope of this report.

5.2. Seismic retrofit of a three-story R/C building

This office building, as the previous one, was originally designed without seismic provisions. Situated in Lisbon, it is composed of three longitudinal and seven transversal three-story R/C frames. A plan, a transversal section, and the cross sections of beams and columns are shown in Fig. 5. Further details on this structure are being published in other deliverables of this Project.
The design simulation is conducted, also in this case, with regard to the transversal direction. A couple of cables, connected to the third floor, is placed on each frame. The assessment enquiry on the unprotected structure at the BDE level (characterised by a peak ground acceleration of 0.27g, according to the Portuguese National Document Application of EN

Eurocode 8) highlighted a maximum inter-story drift of 31.8 mm for second floor (0.91% of story height), from a conventional elastic analysis. However, in this computation a nominal Young modulus of 30000 N/mm^2 was adopted for concrete, corresponding to "uncracked" conditions, for consistency with parallel calculations carried out by other Partners within this research study. A reliable estimate of the modulus for "cracked" conditions could be obtained by dividing the value above by a factor 2 through 3, to which a 2 through 3 amplification of drifts would follow. Moreover, a plastic analysis, herein not developed, would lead to further increased displacements. Therefore, a realistic performance evaluation should locate a maximum inter-story drift around 2.5%-3%. The DCS dimensions are then implicitly calibrated on these data (which also justify a rehabilitation hypothesis), even though all calculations are referred to the "uncracked" Young modulus. This holds true also for the final verification that, for the same reasons, will show very low drifts in protected configuration. But, for the aims of this demonstrative example, these values are to be intended only as comparative terms for proportionally estimating the benefits afforded by the intervention.
As in section 5.1, the design procedure is applied below by following the step-by-step sequence discussed in section 4.

PDP – Step 1

The reference data are: W_s = 4110 kN (corresponding to half structure); T_{1s} = 0.62 s; α_1 = 0.88 (calculated from modal analysis). Then:

(1) $\Rightarrow$ W_s^{m1} = 3617 kN

(2) $\Rightarrow$ K_s^{m1} = 37870 N/mm

By assuming β = 0.8:

(3) $\Rightarrow$ T_{1sdc}^{t} = 0.49 s

(4), (5) $\Rightarrow$ $K_{dc}^{t,h}$ = 22760 N/mm

Being γ_{diag} = 32.8°, from which cosγ_{diag} = 0.839, it follows:

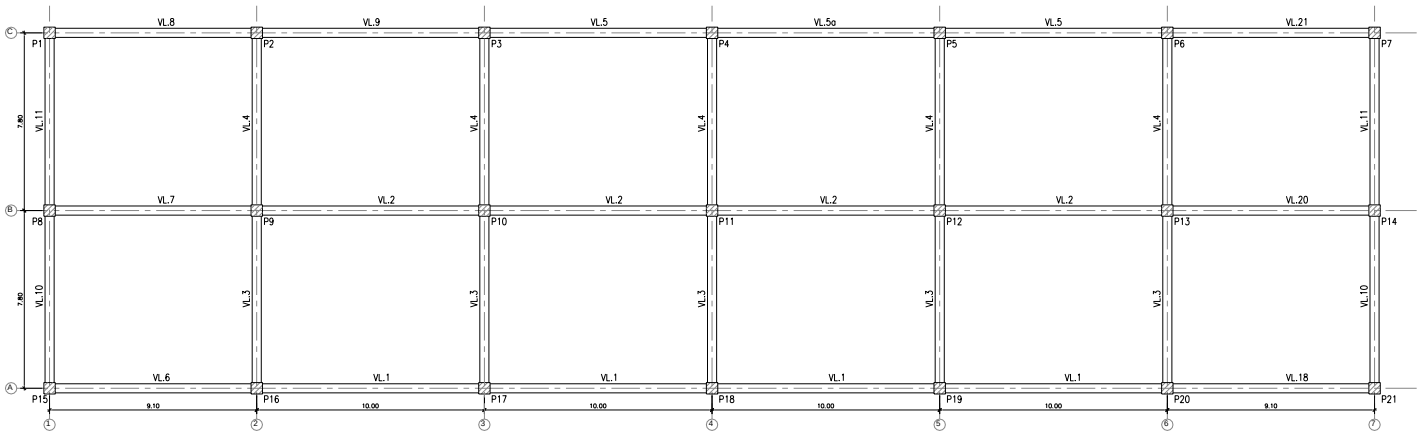

PLAN

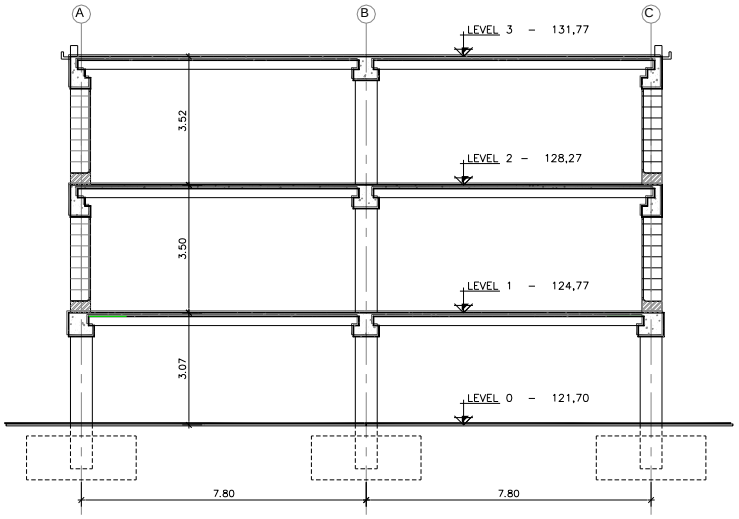

SECTION

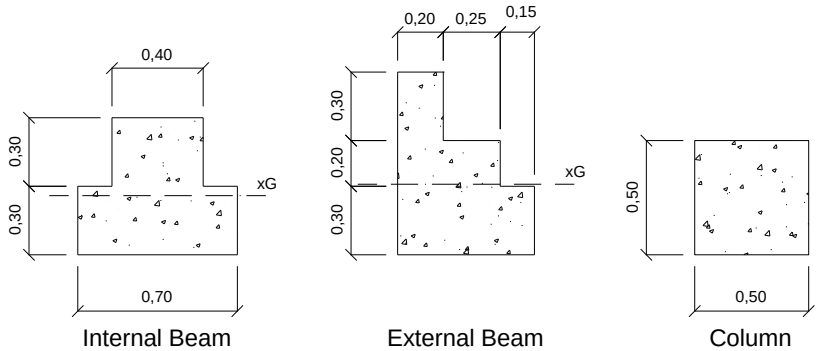

Fig. 4. Plan, transversal section, and frame-member cross sections of three-story R/C building (dimensions in meters)

(6) $\Rightarrow K_{dc}^{t} = \dfrac{K_{dc}^{t,h}}{\cos\gamma_{diag}} = 27130$ N/mm

(8) $\Rightarrow K_{d2}^{t} = K_{c}^{t} = 2K_{dc}^{t} = 54260$ N/mm

The cable layout is traced out by approaching again a parabolic curve, which leads to the geometrical and stiffness data in Table 5.

Floor	L_i (mm)	γ_i (°)	cos(γ_i)	K_{ci}^{p} (N/mm)	$K_{ci}^{p,h}$ (N/mm)
1	8760	20.5	0.936	129452	121167
2	6775	31.1	0.856	167380	143277
3	3864	65.5	0.414	293478	121499

Table 5. Geometrical and stiffness data of cable

From the L_i values in Table 4, $L_t = 19400$ mm, and

(9) $\Rightarrow A_{c}^{t} = \dfrac{K_{c}^{t} \cdot L_{t}}{E_s} = 5100$ mm^2

derive.

Based on (9), three cables of twelve strands are selected, from which $A_{c}^{p} = 5400$ mm^2.

PDP – Step 2

(10) $\Rightarrow K_{c}^{p} = 58460$ N/mm

(11) $\Rightarrow K_{c}^{p,h} = 42620$ N/mm; $K_{dc}^{p,h} = 11875$ N/mm

(12) $\Rightarrow T_{1sdc}^{p} = 0.48$ s

T_{1sdc}^{p} practically coincides with T_{1sdc}^{t}, and thus A_{c}^{p} is confirmed.

(13) $\Rightarrow \cos\gamma_1 = 0.936$; $K_{d2}^{p} = 45530$ N/mm

(14) $\Rightarrow K_{d1}^{p} = 910600$ N/mm

PDP – Step 3

A drift limit of 1% (NS-CP) is assumed, also in this case, as the basic objective of the retrofit design at the MCE level. By referring to the height of the fifth floor (≈ 10 m), d_r = 100 mm is obtained, from which ΔL_c = 84 mm. Then:

(15) $\Rightarrow F_{c0}^{p} = F_{c0}^{p} = 1227$ kN

PDP – Step 4

Based on the preliminarily established cable characteristics, the non-linear dynamic SDOF analysis identifies $C^{p} = 80$ kN/(mm/s)$^{\alpha}$ as the best balance C choice in this case.

FVDP

The final verification phase, carried out by the "J2d" program, substantially validates the results of the PDP. Maximum inter-story drifts of 9.5 mm (0.27%), and 21.7 mm (0.62%) are obtained at the BDE, and MCE levels of input action. These strongly restrained drift values, which highlight a remarkable performance of the designed system, must anyway be kept according to the observations reported at the beginning of this section, with regards to the assessment of the unprotected building.

6. CONCLUSIVE REMARKS

The proposed design procedure showed a remarkable degree of convergence between the predictions of the preliminary phase and the final verification results, with regard to a series

of well-sorted case studies, in addition to the two examples presented herein. Nevertheless, due to its "open-box" conception, further improvements to the involved analytical and empirical relations, as well as different assumptions on relevant tuning coefficients and reference limitations, can be freely introduced in future use.

The two demonstrative retrofit designs were essentially aimed at showing a step-by-step commented application of the procedure, to explain in practice all needed structural transformations and calculations. The DCS characteristics determined for these case studies are anyway to be intended as possible (that is, acceptable in terms of inter-story drift evaluation), but not necessarily final solutions, since no strength-based verification was carried out. Moreover, also a simplified schematisation of the architectural constraints was considered in these analyses.

REFERENCES

[1] Sorace S., Agnolin I., Suraci S., Terenzi G. (2000). *Design and optimisation of damped cable system characteristics to suit application*, Report to European Commission No. EVG1-CT-1999-00013 SPIDER/1.1/UD/SSO/01/ VF-C, Deliverable No. 1, RTD Project SPIDER, November 2000, 54 pp.

[2] Chiarugi A., Krief A., Sorace S., Terenzi G. (2000). *Applicabilità di sistemi di cavi smorzanti per la protezione sismica di strutture intelaiate*, Proceedings of the 13th CTE Italian Conference, Pisa, November 9-11, 2000, CTE, Milan, pp. 573-582.

[3] Sorace S., Terenzi G. (2001). *Deformation and strength-based assessment of damped cable system for seismic retrofit of R/C structures*, Proc. of 5th World Congress on Joints, Bearings and Seismic Systems for Concrete Structures, ACI – ACAI, Rome, October 7-11, 2001, Studio Ega, Rome (CD-ROM).

[4] Sorace S., Rovere N., Suraci S., Terenzi G. (2001). *Development of analysis tools for structures protected by the damped cable system*, Report to European Commission No. EVG1-CT-1999-00013 SPIDER/4.1/UDINE/SSO/02/VF-C, Deliverable No. 8, RTD Project SPIDER, December 2001, 28 pp.

[5] Poggianti A., Welponer A. (2002). *Damper cable system – Analysis of the ENEL-HYDRO structure submitted to different earthquakes*, Report to European Commission

No. EVG1-CT-1999-00013 SPIDER/4.2/ENEA/APO/07/V1-C, Deliverable No. 9, RTD Project SPIDER, April 2002, 12 pp.

[6] Poggianti A., Welponer A. (2002). *Development of a simplified tool for the design of structures equipped with damper cable systems,* Report to European Commission No. EVG1-CT-1999-00013 SPIDER/5.2/ENEA/APO/07/V1-C, Deliverable No. 12, RTD Project SPIDER, May 2002, 20 pp.

[7] Federal Emergency Management Agency – FEMA (1997). *NEHRP Guidelines for the seismic rehabilitation of buildings*, FEMA Report No. 273, Washingthon, DC.

[8] Federal Emergency Management Agency – FEMA (1997). *NEHRP Commentary on the seismic rehabilitation of buildings*, FEMA Report No. 274, Washingthon, DC.

[9] Applied Technology Council – ATC (1996). *Seismic evaluation and retrofit of concrete buildings*, ATC Report No. 40, Redwood City, CA.

[10] Structural Engineers Association of California – SEAOC (2000). Guidelines for performance-based seismic engineering, SEAOC Blue Book, Appendix I.

[11] Computers & Structures Inc. (1997). *SAP200NL: Structural Analysis Programs*, Version No. 6.11, Theoretical and Users Manual, Berkeley, CA.